The decay of the pair correlation function in simple fluids: long- versus short-ranged potentials

1994 J. Phys.: Condens. Matter 6 9275

(http://iopscience.iop.org/0953-8984/6/44/008)

J. Phys.: Condens. Matter 6 (1994) 9275–9294. Printed in the UK

The decay of the pair correlation function in simple fluids: long- versus short-ranged potentials

R J F Leote de Carvalho†, R Evans†, D C Hoyle† and J R Henderson‡
† H H Wills Physics Laboratory, University of Bristol, Bristol BS8 1TL, UK
‡ School of Chemistry, University of Leeds, Leeds LS2 9TJ, UK

Received 12 August 1994

Abstract. This paper is concerned with two aspects of the theory of the decay of $g(r)$, the radial distribution function of a liquid. For models in which the attractive interatomic potential is short ranged, asymptotic decay falls generically into two classes: (a) monotonic decay for which $r(g(r)-1) \sim \exp(-\alpha_0 r)$ and (b) damped oscillatory decay for which this function $\sim \exp(-\tilde{\alpha}_0 r)\cos(\alpha_1 r - \theta)$. Crossover between the two classes ($\alpha_0 = \tilde{\alpha}_0$) defines the Fisher–Widom line of the particular model. This line is calculated for a truncated Lennard-Jones fluid using an accurate (HMSA) integral-equation theory. We find that it intersects the liquid branch of the liquid–vapour coexistence curve at $T/T_c \approx 0.9$ and $\rho/\rho_c \approx 1.9$, where T_c and ρ_c are the critical temperature and density, respectively. The location of the line relative to coexistence is very similar to that calculated earlier using the random phase approximation (RPA) for a square-well fluid, suggesting that in this region it is not particularly sensitive to choice of potential or of theory. In the second part of the paper we develop a theory for the intermediate-range and asymptotic decay of $g(r)$ for a fluid whose potential includes power-law (dispersion) contributions. Although power-law decay dominates at longest range, we show that intermediate-range oscillatory structure is determined by a single complex pole. Explicit calculations, within the RPA, for a model potential with a $1/r^6$ tail show that at high densities this pole is located close to that of a reference model with a short-ranged truncated potential and the intermediate- and short-range structure of the two models is almost identical. However, since there is no pure imaginary pole for the long-ranged potential, there is no pure exponential decay of correlations and, therefore, no sharply defined Fisher–Widom line. Intermediate-range oscillations in $g(r)$ are eroded at lower densities but the mechanism is different from that in the short-ranged models. In addition, we find that the pole structure of models with large truncation lengths is very different from that of the full potential making asymptotic analysis for such models of little practical use.

1. Introduction

Medium-range and asymptotic correlations in liquids and their mixtures control important aspects of interfacial phase behaviour, relevant to, for example, wetting phenomena, capillary condensation and the solvation of colloidal particles [1, 2, 3, 4]. This observation has inspired the development of a general theoretical framework for describing the decay of inhomogeneous fluid structure in terms of the pair correlations of a bulk fluid [2, 3, 4, 5]. In order to understand interfacial behaviour one needs to understand the nature of the decay of $g(r)$, the radial distribution function of the appropriate bulk fluid. The latter is most readily described via the behaviour of the complex Fourier transform of the bulk direct correlation function, $\hat{c}(q)$. For model fluids with short-ranged potentials the functional form of intermediate-range correlations and the asymptotic decay of $g(r)$ is determined by the pole structure of the liquid structure factor $S(q)$, i.e., by solutions q of $1-\rho\hat{c}(q)=0$, where

0953-8984/94/449275+20$19.50

ρ denotes density, with the smallest imaginary part (reviewed in subsection 2.1 below). If the leading-order solution is purely imaginary then the asymptotic decay of $r(g(r)-1)$ is exponential; otherwise one obtains the familiar exponentially damped oscillatory form. The line in (ρ, T) space (T denotes temperature) where the decay changes from one form to the other is known as the Fisher–Widom (FW) line [6, 3, 2]. In subsection 3.1 below we present what we believe is the first calculation of the position of the FW line based on a highly accurate integral-equation theory of simple liquids. The results, for a truncated Lennard-Jones fluid, confirm earlier predictions based on the RPA for the square-well fluid [3], that the FW line crosses the liquid branch of the liquid–vapour coexistence curve at $T/T_c \approx 0.9$. Furthermore they confirm that asymptotic forms provide a remarkably accurate description of intermediate-range correlations, i.e., of $g(r)$ for $r \gtrsim 2\sigma$.

While computer simulators are usually forced to employ truncated potentials, nature insists that dispersion forces are truly long ranged. The consequences of such forces for interfacial properties was recognized by Derjaguin and his school in the 1930s. Their implications for the asymptotic behaviour of $g(r)$ were first recognized by Widom [7] and Enderby *et al* [8]. The latter authors showed that if the pairwise potential $\phi(r)$ has power-law decay then $g(r)-1 \to -S^2(0)\phi(r)/k_BT$ as $r \to \infty$, with $S(0) = \rho k_B T \chi_T$, where χ_T is the isothermal compressibility. At intermediate range, where one still expects to observe damped oscillations in $g(r)$, the role of dispersion (power-law) forces is less clear. Verlet [9] appears to have been the first to note the difficulty in separating intermediate-range structure from long-range power-law decay. Power-law asymptotics are determined not by solutions of $1-\rho\hat{c}(q)=0$ but rather by terms in the small-q expansion of $\hat{c}(q)$ that are non-analytic in q^2 [8]. However, recent work [2] has speculated that the former continues to control the nature of intermediate-range oscillatory correlations. Subsection 2.2 below presents a formal approach to obtaining both the intermediate-range and asymptotic decay of the radial distribution functions of models that incorporate power-law interactions. In particular, we obtain a separation between power-law r^{-6} decay of $g(r)-1$ controlled (at leading-order) by a q^3 term in $\hat{c}(q)$ and oscillatory structure arising from solutions of $1-\rho\hat{c}(q)=0$ at complex q. This leads to a formula (23) for the intermediate and asymptotic behaviour of $g(r)$ for a pairwise potential decaying as $-a_6/r^6$. In subsection 3.2 we examine the usefulness of this formula for a simple model treated in the RPA. For high densities, we find that retaining the leading-order (oscillatory) pole contribution plus the slowest-decaying power law (see (38)) provides a very accurate description of both the intermediate-range and asymptotic behaviour of the 'exact' $g(r)$ obtained from the full solution of the RPA. Thus, we believe that (23) (or its simplified version (38)) constitutes the description of intermediate-range-oscillatory correlations competing with power-law tails that Verlet [9] was seeking. In addition, we consider the pole structure and, hence, the asymptotic correlations of truncated (finite-ranged) versions of the same model with increasing truncation lengths. Our results enable us to ascertain what remains of the FW line mechanism, controlling the onset of oscillatory decay in short-ranged models, when power-law interactions are included. Other aspects of our results are discussed in section 4.

2. Theory

The Ornstein–Zernike (OZ) integral equation defines the functional inversion between the total pair correlation function $h(r) \equiv g(r) - 1$ and the direct correlation function $c(r)$. For

pure fluids it is written in real space as

$$h(r) = c(r) + \rho \int \mathrm{d}r'\, h(r')\, c(|r - r'|) \tag{1}$$

and in Fourier space as

$$\hat{h}(q) = \frac{\hat{c}(q)}{1 - \rho\hat{c}(q)} \tag{2}$$

with ρ the bulk density, where the Fourier transform of a function $f(r)$ is

$$\hat{f}(q) = 4\pi \int_0^\infty \mathrm{d}r\, r^2 f(r) \frac{\sin qr}{qr}. \tag{3}$$

The inverse Fourier transform is then

$$f(r) = \frac{1}{2\pi^2} \int_0^\infty \mathrm{d}q\, q^2 \hat{f}(q) \frac{\sin qr}{qr}. \tag{4}$$

In analysing the asymptotics of $h(r)$ we must distinguish between fluids for which $c(r)$ is short ranged (finite ranged or exponentially decaying) and those for which $c(r)$ decays as a power law.

2.1. Asymptotics of $h(r)$: short-ranged case

The asymptotic decay of correlations for short-ranged interatomic potentials was considered elsewhere [2, 3] and here we merely summarize the relevant results.

If the system is characterized by an interatomic pair potential $\phi(r)$ that is finite ranged or exponentially decaying, i.e., $c(r)$ decays faster than a power law†, then $\hat{c}(q)$ possesses a small-q Taylor expansion about $q = 0$

$$\hat{c}(q) = c^{(0)} + c^{(2)}q^2 + c^{(4)}q^4 + c^{(6)}q^6 + \ldots. \tag{5}$$

Since $\hat{c}(q)$ is even all odd derivatives must vanish for $q = 0$ and the moments in the Taylor expansion (5), defined in terms of the even derivatives, are all finite and are given by

$$c^{(2n)} = \frac{4\pi(-1)^n}{(2n+1)!} \int_0^\infty \mathrm{d}r\, c(r) r^{2n+2}. \tag{6}$$

Although $c(r)$, $h(r)$ and their Fourier transforms $\hat{c}(q)$ and $\hat{h}(q)$ have physical meaning for real $r \geqslant 0$ and $q \geqslant 0$ only, it is convenient to consider $\hat{c}(q)$ and $\hat{h}(q)$ for q in the complex plane. Since $\hat{h}(q)$ is an even function of q

$$rh(r) = \frac{1}{2\pi^2} \int_0^\infty \mathrm{d}q\, q \sin qr\, \hat{h}(q) = \frac{1}{4\pi^2 \mathrm{i}} \int_{-\infty}^\infty \mathrm{d}q\, q\, \mathrm{e}^{\mathrm{i}qr} \frac{\hat{c}(q)}{1 - \rho\hat{c}(q)} \tag{7}$$

† We exclude the region of the bulk critical point.

and we expect $\hat{h}(q)$ to exhibit poles at complex $q = \alpha \equiv \alpha_1 + i\alpha_0$ satisfying

$$1 - \rho\hat{c}(\alpha) = 0. \tag{8}$$

There can be no poles lying on the real axis apart from the liquid–vapour spinodals ($\alpha = 0$) and an infinite-ranged oscillatory solution often found at very high density ($\alpha_0 = 0$, $\alpha_1 \neq 0$) [5]. A pole can lie on the imaginary axis where it gives rise to pure exponential decay of $rh(r)$ [2]. Other poles lie off the imaginary and real axes where they give rise to exponentially damped oscillatory decay [2, 3]. In the latter case poles must occur in conjugate pairs $\alpha = \pm\alpha_1 + i\alpha_0$. Equating real and imaginary parts in (8) we have

$$1 = 4\pi\rho \int_0^\infty dr\, r^2 c(r) \frac{\sinh(\alpha_0 r)}{\alpha_0 r} \cos(\alpha_1 r) \tag{9}$$

$$1 = 4\pi\rho \int_0^\infty dr\, r^2 c(r) \cosh(\alpha_0 r) \frac{\sin(\alpha_1 r)}{\alpha_1 r}. \tag{10}$$

When $c(r)$ is of finite range this pair of equations can always be used to solve for α_0 and α_1. Caution must be exercised when $c(r)$ decays exponentially because, depending on its decay length, the integrals may or may not exist. A pure imaginary pole $q = i\alpha_0$ is obtained from (9) alone with $\alpha_1 = 0$. The right-hand side of (7) can be evaluated by contour integration. Choosing an infinite-radius semicircle in the upper half-plane we obtain

$$rh(r) = \frac{1}{2\pi} \sum_n e^{iq_n r} R_n = \sum_n e^{iq_n r} A_n \tag{11}$$

where q_n is the nth pole, R_n is the residue of $q\,\hat{c}(q)/\left(1 - \rho\hat{c}(q)\right)$ at $q = q_n$ and $A_n = R_n/2\pi$ is a (complex) amplitude. For the model potentials and closures that have been studied there is an infinite number of poles. It is assumed that the integrand always vanishes on the outer arc of the contour. For large r, $h(r)$ is determined by the pole or poles with the smallest inverse decay length α_0. Two scenarios arise: (a) a pole lying on the imaginary axis has the lowest value and the ultimate decay is purely exponential; and (b) a conjugate pair of poles has a smaller α_0 than that of the pole on the imaginary axis and the ultimate decay is exponentially damped oscillatory. The FW line in the (ρ, T) plane is where the conjugate pair of poles closest to the real axis has the same α_0 as the pole on the imaginary axis [2, 3].

If we assume that all poles are simple then the residues are given by

$$R_n = -q_n/\rho^2\hat{c}'(q_n) \tag{12}$$

where prime denotes derivative WRT q. A pole on the imaginary axis $q_n = i\alpha_0$ makes a contribution $A\,e^{-\alpha_0 r}$ to $rh(r)$ where $A = -i\alpha_0/2\pi\rho^2\hat{c}'(i\alpha_0)$ is the amplitude. A pair of conjugate poles $q_n = \pm\alpha_1 + i\alpha_0$ makes a contribution $2|A|\,e^{-\alpha_0 r}\cos(\alpha_1 r - \theta)$ where $|A|\,e^{-i\theta} = -\alpha/2\pi\rho^2\hat{c}'(\alpha)$ with positive α_1 and θ defined by the right-hand pole [2].

2.2. Asymptotics of $h(r)$: long-ranged case

In real fluids long-ranged forces are always present and these have a profound effect on the ultimate asymptotics of correlation functions. When long-range (van der Waals) interactions are taken into account the pairwise potential decays as $\phi(r) \sim a_n/r^n$ with n positive. These are usually divided into three classes: electrostatic, dipolar and dispersion (London) forces. We consider only the case of dispersion (London) forces. The asymptotics of correlation functions for ionic fluids was analysed very recently by several groups [10].

In an atomic fluid, the leading dispersion term is $(-a_6/r^6)$, with $a_6 > 0$. This describes the instantaneous induced-dipole–induced-dipole interaction. Higher-order terms represent dipole–quadrupole $(-a_8/r^8)$, quadrupole–quadrupole $(-a_{10}/r^{10})$ interactions, and so on. These latter contributions are, in general, small when compared with the term r^{-6} [11]. For large separations retardation becomes important and the leading-order r^{-6} decay crosses over to r^{-7} decay. The implications of such crossover for the behaviour of $\hat{h}(q)$ at small q has been discussed recently by Reatto and Tau [12]. Here we restrict consideration to the case of a model fluid where the only power-law contribution to $\phi(r)$ is the term $-a_6/r^6$ and this term is not modified at larger r. Incorporating extra power-law contributions and crossover complicates the analysis. We return to this point later.

Outside the bulk critical region, it is known from diagrammatic analysis that $c(r) \to -\beta\phi(r) \sim \beta a_6/r^6$ when $r \to \infty$, where $\beta = 1/k_B T$. Thus, all moments of $c(r)$ with $n \geqslant 2$, defined as in (6), diverge at the upper limit and the small-q Taylor expansion (5) is no longer valid.

The presence of an r^{-6} interaction also invalidates the approach based on equations (9) and (10) for finding the poles, since the integrals diverge. This does not mean that poles do not exist. Rather alternative procedures must be found for locating the zeros of $1 - \rho\hat{c}(q)$. Once the poles are determined there will be an expansion, of the form (11), in terms of complex exponentials. In addition we now expect power-law contributions to the decay of $h(r)$. A satisfactory description of the asymptotics of $h(r)$ must combine both types of contribution. What we know from integral equation studies of full Lennard-Jones (LJ) 12–6 fluids is that the short- to intermediate-ranged correlations, i.e., the oscillatory parts of $h(r)$, appear to be essentially the same as those in fluids with a truncated LJ potential. This suggests that the leading-order complex poles make much the same contribution for both types of fluid. In order to investigate this conjecture and the possible relevance of pole structure to intermediate-range correlations in fluids with long-ranged potentials it is natural to consider [2] two possible approaches: (a) use of truncated (finite-ranged) potentials of increasingly long-range, (b) use of perturbation theory to separate out the effects of a true power-law term. As we discuss further in subsection 3.2, approach (a), though interesting in its own right, is not particularly convenient or revealing. As we increase the cut-off distance poles cluster along a line and move down towards the real axis. The poles are no longer well separated and the pole analysis, though formally correct, is not very useful. More and more terms are required in (11) in order to achieve a reliable description of the asymptotics. Approach (b) takes a different standpoint. It argues [2] that by making a suitable choice of finite-ranged reference potential it should be possible to mimic very accurately short- to intermediate-range correlations, i.e., the reference $h(r)$ should be very close to $h(r)$ of the full $\phi(r)$, except at very long range where the known power-law decay takes over. We examine this conjecture further in subsection 3.2.

Our aim in the remainder of the section is to develop an explicit asymptotic expansion for $h(r)$. By returning to the basic theory and selecting a convenient contour in the complex plane we obtain an expansion in terms of complex exponentials (from poles) plus a series expansion in inverse powers of r.

The key feature arising from the $-a_6/r^6$ potential is the presence of a q^3 term in the Fourier transform of the direct correlation function [8, 13]. Asymptotic Fourier analysis [8, 14] shows that if $c(r) \to -\beta\phi(r)$, as $r \to \infty$, then the small-q Taylor expansion of $\hat{c}(q)$ must contain a q^3 term. We assume for positive real q that $\hat{c}(q)$ can be expressed as

$$\hat{c}(q) = \hat{c}^{\,\mathrm{sr}}(q) + aq^3 \tag{13}$$

where

$$a = \beta a_6 \pi^2/12 \tag{14}$$

and $\hat{c}^{\,\mathrm{sr}}(q)$ is the Fourier transform of a short-ranged function possessing an expansion in powers of q^2

$$\hat{c}^{\,\mathrm{sr}}(q) = c^{\mathrm{sr}(0)} + c^{\mathrm{sr}(2)}q^2 + c^{\mathrm{sr}(4)}q^4 + \ldots. \tag{15}$$

Note that (13) applies to the entire real axis only if the q^3 term is multiplied by $\mathrm{sgn}(q)$, which ensures that $\hat{c}(q)$ is an even function of q. It is not immediately apparent that $\hat{c}(q)$ should take the form (13). Within the random phase approximation (RPA), (13) follows explicitly [13]. That is, if we assume that the only inverse power-law contribution to $c(r)$ is the term $\beta a_6/r^6$ then the only term in $\hat{c}(q)$ which is non-analytic in q^2 is the q^3 term [8, 13]. Closure approximations which go beyond the RPA could introduce corrections $O(h^2(r))$ into the tail of $c(r)$—see, e.g., the HNC asymptotic result (30). These correspond to terms $O(r^{-12})$ which would then give rise to a q^9 term in $\hat{c}(q)$. We do not consider these in the present analysis.

It is easy to see that the analysis carried out for the short-ranged case is no longer valid when there is a q^3 term in $\hat{c}(q)$. (This term is in fact responsible for the ultimate algebraic decay of $h(r)$ [13].) By choosing the contour around the upper right quadrant of the complex plane and closing along the imaginary axis $q = \mathrm{i}\alpha_0$ we have

$$rh(r) = \frac{1}{2\pi^2}\mathrm{Im}\left[\int_0^\infty \mathrm{d}q\, q\mathrm{e}^{\mathrm{i}qr}\frac{\hat{c}(q)}{1-\rho\hat{c}(q)}\right] = \frac{1}{2\pi^2}\mathrm{Im}\left[2\pi\mathrm{i}\sum_n \mathrm{e}^{\mathrm{i}q_n r}R_n + \int_0^\infty \mathrm{d}(\mathrm{i}\alpha_0)\,\mathrm{i}\alpha_0\,\mathrm{e}^{-\alpha_0 r}\frac{\hat{c}(\mathrm{i}\alpha_0)}{1-\rho\hat{c}(\mathrm{i}\alpha_0)}\right] \tag{16}$$

where q_n is the nth pole in the first quadrant and R_n the residue of $q\,\hat{c}(q)/\left(1-\rho\hat{c}(q)\right)$ at $q = q_n$. These poles are given by the zeros of the denominator

$$0 = 1 - \rho\hat{c}(q) = 1 - \rho\left(\hat{c}^{\,\mathrm{sr}}(q) + aq^3\right). \tag{17}$$

As in the short-ranged case, all poles must lie off the real axis except for those corresponding to infinite range correlations, such as occur at the spinodals and critical point. However, now there can be no poles on the imaginary axis. To see this, we assume that $q = \mathrm{i}\alpha_0$ is a

pure imaginary solution of (17), then, since $\hat{c}^{sr}(q)$ is even, $\hat{c}^{sr}(i\alpha_0)$ is real. Taking real and imaginary parts in (17) requires

$$0 = 1 - \rho\hat{c}^{sr}(i\alpha_0) \qquad 0 = i\rho a\alpha_0^3 \tag{18}$$

which can only have the solution $\alpha_0 \equiv 0$. Thus, all poles must lie off both the real and the imaginary axes.

As before, we assume the poles $q = \alpha_1 + i\alpha_0$ are simple. Then the residues are given by (12). A pole makes a contribution $|A_n|\,e^{-\alpha_0^n r}\cos(\alpha_1^n r - \theta_n)$ where the complex amplitude is defined as

$$A_n = |A_n|\,e^{-i\theta_n} = R_n/\pi. \tag{19}$$

It remains to evaluate the integral in (16). This can be re-written as

$$\begin{aligned} I &= -\frac{1}{2\pi^2}\mathrm{Im}\left[\int_0^\infty d\alpha_0\,\alpha_0\,e^{-\alpha_0 r}\left(-\frac{1}{\rho}\right)\left(1 - \frac{1}{1-\rho\hat{c}(i\alpha_0)}\right)\right] \\ &= -\frac{1}{2\pi^2\rho}\mathrm{Im}\left[\int_0^\infty d\alpha_0\,\alpha_0\,e^{-\alpha_0 r}\left(\frac{1}{1-\rho\left(\hat{c}^{sr}(i\alpha_0) + a(i\alpha_0)^3\right)}\right)\right] \end{aligned} \tag{20}$$

where we have dropped a real integral. The remaining integral is dominated by the small-α_0 region. Expanding $\hat{c}^{sr}(i\alpha_0)$ as in (15) we obtain

$$\begin{aligned} I = -\frac{1}{2\pi^2\rho}\mathrm{Im}\Bigg[&\int_0^\infty d\alpha_0\left(\frac{\alpha_0\,e^{-\alpha_0 r}}{1-\rho c^{sr(0)}}\right) \\ &\times\left(\frac{1}{1-\rho\left(-c^{sr(2)}\alpha_0^2 + c^{sr(4)}\alpha_0^4 - c^{sr(6)}\alpha_0^6 + \ldots - ia\alpha_0^3\right)/(1-\rho c^{sr(0)})}\right)\Bigg]. \end{aligned} \tag{21}$$

Finally, by expanding the second factor and retaining only the imaginary contributions we obtain the desired inverse power series

$$\begin{aligned} I &= -\frac{1}{2\pi^2\rho}\int_0^\infty d\alpha_0\,\alpha_0\,e^{-\alpha_0 r}\left(\frac{-\rho a\alpha_0^3}{(1-\rho c^{sr(0)})^2} + O(\alpha_0^5)\right) \\ &= \frac{a}{2\pi^2}\frac{1}{(1-\rho c^{sr(0)})^2}\int_0^\infty d\alpha_0\,e^{-\alpha_0 r}(\alpha_0^4 + O(\alpha_0^6)) \\ &= \frac{a}{2\pi^2}S^2(0)\left(\frac{4!}{r^5} + O\left(\frac{1}{r^7}\right)\right) = \frac{12aS^2(0)}{\pi^2}\frac{1}{r^5} + O\left(\frac{1}{r^7}\right) \\ &= \beta a_6 S^2(0)\frac{1}{r^5} + O\left(\frac{1}{r^7}\right) \end{aligned} \tag{22}$$

where $S(0)$ is the structure factor $S(q) \equiv 1 + \rho\hat{h}(q) = 1/(1-\rho\hat{c}(q))$ at $q = 0$. The first term in the inverse power-series expansion for $rh(r)$ is identical to the result in [8] and

coefficients of higher-order terms are easily obtained from (21). Note that I would vanish if $\hat{c}(q)$ contained only even powers of q which is, of course, the case for a short-ranged potential.

Combining the power series with pole contributions yields the final asymptotic form

$$rh(r) = \sum_n |A_n| \, e^{-\alpha_0^n r} \cos(\alpha_1^n r - \theta_n) + S^2(0)\beta\frac{a_6}{r^5} + \text{HO} \tag{23}$$

where the bound of the higher order terms can only be proved to be $O(1/r^7)$. One can show that there cannot be any exponential terms in the omitted higher order terms. Equation (23) is a key result of the paper. The most significant difference between short- and long-ranged cases is the replacement of monotonic exponentially decaying terms due to pure imaginary poles by the series expansion in inverse powers of r. As a consequence no sharp FW line can be defined in the long-ranged case, since there can be no crossover from pure exponential to damped oscillatory decay at any range. The ultimate decay of $h(r)$ is $\beta a_6 S^2(0)/r^6$ for all fluid states away from the critical point and the spinodals. However, this does not mean that *intermediate-range* structure will not reflect the thermodynamic state. In particular, as the density is decreased at fixed T, $S(0)$ ($\propto \chi_T$) typically increases rapidly and we expect power-law decay to set in at smaller separations thereby eroding the oscillatory (pole) contributions to $h(r)$. This is illustrated in subsection 3.2 where we examine the usefulness of (23) in accounting for correlations at intermediate range.

3. Results of calculations

3.1. Short-ranged case

Here we present results for the asymptotics of $h(r)$ for a soft-core finite-ranged potential treated within an accurate theory. We have chosen to work with the Lennard-Jones 6–12 potential truncated and shifted at 2.5σ

$$\begin{aligned} \phi_{\text{LJts}}(r) &= \phi_{\text{LJ}}(r) - \phi_{\text{LJ}}(R) \quad r \leqslant R \\ &= 0 \qquad\qquad\qquad\quad r > R \end{aligned} \tag{24}$$

where $R = 2.5\sigma$ and $\phi_{\text{LJ}}(r) = 4\epsilon((\sigma/r)^{12} - (\sigma/r)^6)$. The liquid–vapour coexistence curve for this potential was determined using the Gibbs-ensemble simulation method by Smit [15] and the estimates of reduced critical temperature and density are respectively $T_c^* = 1.085$ and $\rho_c^* = 0.32$. The minimum of the potential occurs at $r = 2^{1/6}\sigma$ and so its WCA [16] division is

$$\begin{aligned} \phi_0(r) &= \phi_{\text{LJts}}(r) - \phi_{\text{LJts}}(2^{1/6}\sigma) \qquad r \leqslant 2^{1/6}\sigma \\ &= 0 \qquad\qquad\qquad\qquad\qquad\quad r > 2^{1/6}\sigma \end{aligned} \tag{25}$$

for the repulsive part and

$$\begin{aligned} \phi_1(r) &= \phi_{\text{LJts}}(2^{1/6}\sigma) \qquad r \leqslant 2^{1/6}\sigma \\ &= \phi_{\text{LJts}}(r) \qquad\qquad\quad r > 2^{1/6}\sigma \end{aligned} \tag{26}$$

for the remaining part.

In our calculations we have employed the Zerah and Hansen [17] HMSA closure to the OZ integral equation (1)

$$\ln(h(r)+1) = -\beta\phi_0(r) + \ln\left(1 + \frac{\exp[\tau(r)(h(r)-c(r)-\beta\phi_1(r))]-1}{\tau(r)}\right). \tag{27}$$

The switching function $\tau(r) \equiv 1 - e^{-\tilde{\alpha}r}$ depends on a single parameter $\tilde{\alpha}$ and interpolates between the soft-mean-spherical approximation (SMSA) closure when $\tilde{\alpha}r \to 0$ ($\tau(r) \to 0$)

$$\ln(h(r)+1) = -\beta\phi_0(r) + \ln(1 + h(r) - c(r) - \beta\phi_1(r)) \tag{28}$$

and the hypernetted-chain (HNC) closure when $\tilde{\alpha}r \to \infty$ ($\tau(r) \to 1$)

$$\ln(h(r)+1) = -\beta\phi(r) + h(r) - c(r). \tag{29}$$

The mixing parameter $\tilde{\alpha}$ is a function of density and temperature and is chosen so as to impose self-consistency between the virial and compressibility routes to the equation of state [17]. We have used a standard Picard iterative method with under-relaxation and fast Fourier transforms to solve the HMSA. At each thermodynamic state $\tilde{\alpha}$ is determined by requiring the isothermal compressibility χ_T calculated by numerical differentiation of the virial pressure WRT the density to agree with that calculated from the fluctuation theorem: $\rho\chi_T = \beta S(0)$.

The HMSA was used recently by Caccamo *et al* [18] in the study of phase-stability of the LJ fluid†. They assessed the residual inconsistency between the virial and energy routes for several representative states in the phase diagram and concluded that imposing self-consistency between the virial and compressibility routes is sufficient to ensure a good degree of consistency among all three routes to the thermodynamics. Moreover, they found remarkable agreement between simulation data and HMSA calculations for the liquid–vapour coexistence curve. The HMSA was also used by Abramo and Caccamo [19] and by Cheng *et al* [20] to predict the phase diagram of a two-component LJ fluid and the rigid C_{60} fluid, respectively. A growing body of evidence suggests that the HMSA is one of the most reliable and accurate integral-equation theories of liquids.

Expanding $\ln(h(r)+1) \sim h(r) - \frac{1}{2}h^2(r) + \ldots$ in (29) it follows that the asymptotic decay of $c(r)$, in the HNC theory, is

$$c(r) \sim -\beta\phi(r) + \tfrac{1}{2}h^2(r) + \ldots \tag{30}$$

i.e., $c(r) \neq 0$ for $r > R$. By contrast, within the SMSA (28) $c(r) = -\beta\phi_1(r)$ for r beyond the range of $\phi_0(r)$ so that $c(r) = 0$ for $r > R$. The HMSA (27), with $0 < \tau(r) < 1$, yields

$$c(r) \sim -\beta\phi_1(r) + \tau(r)\tfrac{1}{2}h^2(r) + \ldots. \tag{31}$$

† A large cut-off $R = 14\sigma$ was employed in [18].

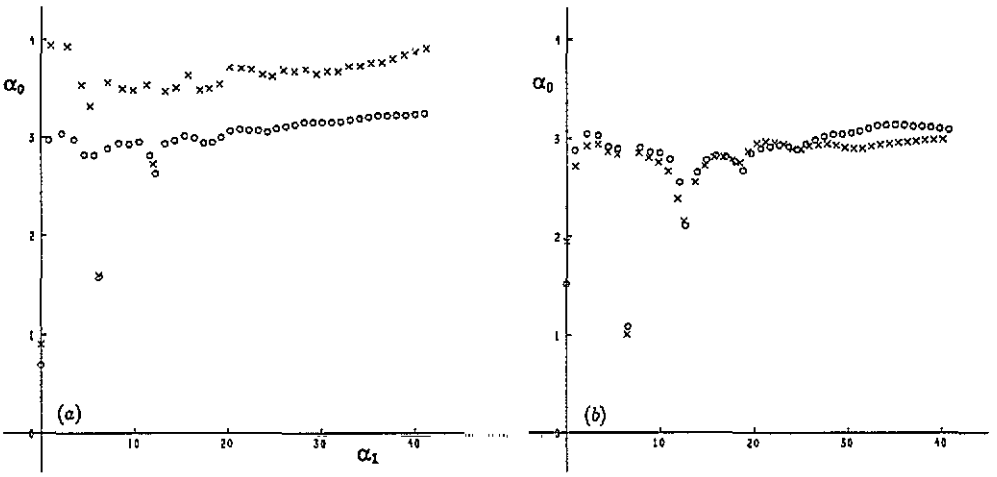

Figure 1. The poles of $\hat{h}(q)$ for the truncated and shifted LJ fluid at $T^* = 1.2$ for two densities (a) $\rho^* = 0.445$ and (b) $\rho^* = 0.715$. The crosses refer to HMSA results and the circles to HNC results. Poles off the imaginary axis occur in conjugate pairs $\alpha = \pm\alpha_1 + i\alpha_0$. Only those with $\alpha_1 > 0$ are shown here and there is an infinite number lying at higher values of α_1 than those plotted. α_0 and α_1 are in units of σ^{-1}.

Thus, the slowest asymptotic decay ($\tau(r) \equiv 1$) that can occur is $c(r) \sim \frac{1}{2}h^2(r) \sim O\left(e^{-2\alpha_0 r}\right)$. This implies that the integrals in equations (9) and (10) are not divergent and therefore these can be used for determining the poles. We have determined the poles $\alpha = \pm\alpha_1 + i\alpha_0$ of $\hat{h}(q)$ from these equations for both the HNC and the HMSA theories. In figure 1 we plot the real and imaginary parts of the poles for the supercritical temperature $T^* = 1.2$. In figure 1(a) the density is $\rho^* = 0.445$ and in figure 1(b) it is $\rho^* = 0.715$. The mixing parameter $\tilde{\alpha}$ for self-consistency of the HMSA theory is $\tilde{\alpha} = 0.795$ and $\tilde{\alpha} = 0.220$, respectively. These plots should be compared with those in figure 2 in [2] where the poles for the square-well fluid treated in the RPA are shown. Although the results for the hard-core fluid in the crude RPA differ in detail from those given here for the soft-core fluid in the more sophisticated HNC and HMSA theories, there are important similarities. In particular, in all three cases the poles closest to the real axis are a single pole on the imaginary axis and a conjugate pair of complex poles with $\alpha_1 \approx 2\pi/\sigma$. These are the poles which give the dominant asymptotic contributions. The difference between the present results and those for the square-well fluid in the RPA lies in the presence of many more poles at higher values of α_0, reflecting a different class of short-range structure. The two plots in figure 1 were chosen to lie on opposite sides of the FW line in the (ρ,T) plane. At the lower density, figure 1(a), the pure imaginary pole has the lower value of α_0, whereas at the higher density, figure 1(b), the complex pole has the lower value. While the value of α_0 for the pure imaginary pole does depend considerably on the choice of closure approximation the location of the leading complex pole appears insensitive

It is tedious but straightforward to map out the FW line in the (ρ,T) plane. The HMSA results, for $R = 2.5\sigma$, are shown in figure 2, along with the liquid–vapour coexistence curve obtained from simulation [15]. We did not attempt to calculate the coexistence curve using the HMSA, as the implementation of the self-consistency criteria of the HMSA makes this a very time-consuming process. However, from the results reported in [18] we would expect the HMSA results for the present potential to be close to those of simulation since

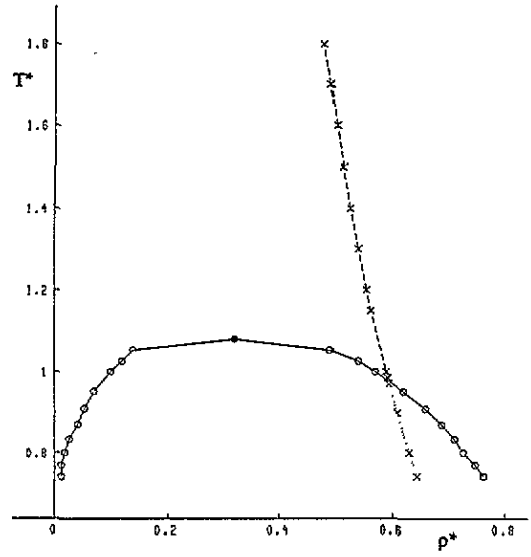

Figure 2. The FW line (crosses) for the truncated and shifted LJ fluid calculated from the HMSA. On the dashed portion of this line the pressure is positive, whereas on the dotted portion it is negative. The solid line joining circles denotes the simulation results [15] for the liquid–vapour coexistence curve. The solid circle is the simulation estimate of the critical point.

only the value of R has changed. Support for this assertion comes from the fact that the pressure obtained from the HMSA is positive on the dashed branch of the FW line plotted in figure 2, appropriate to the single-phase region, but is negative on the dotted branch, which lies inside the simulation coexistence curve. On the left-hand side of the FW line in figure 2 the imaginary pole $i\alpha_0$ dominates at longest range and the decay of $rh(r)$ is monotonic exponential. On the right-hand side the conjugate pair of poles $\pm\alpha_1 + i\alpha_0$ with $\alpha_1 \approx 2\pi/\sigma$ dominates at longest range and the ultimate decay of $rh(r)$ is exponentially damped oscillatory.

The present results should be compared with those in [3] (see figure 2 in [3]) for the square-well fluid treated in the RPA. The present FW line has the same location with respect to the coexistence curve as that in [3]. It intersects the liquid side at $T/T_c \approx 0.90$ and $\rho/\rho_c \approx 1.87$. The corresponding results in [3] are $T/T_c \approx 0.90$ and $\rho/\rho_c \approx 1.92$. Moreover, we find that on the FW line the linear relation

$$\alpha_0\sigma = -a_1\rho\sigma^3 + b_1 \tag{32}$$

where a_1 and b_1 are positive constants is obeyed reasonably well throughout the range of the HMSA calculations, i.e., for $0.7 \lesssim T/T_c \lesssim 1.7$. A similar linear relation was found in the earlier treatment—see (6) of [3]. However, whereas the value of a_1 appears insensitive, the result for b_1 differs significantly from the square-well RPA result. The FW line deviates from that in the square-well RPA at much higher T, with the latter crossing the critical density at a significantly lower temperature ($T/T_c \sim 1.8$) than what is suggested by extrapolation of the present line in figure 2. Of course, as $T \to \infty$ these models should exhibit properties characteristic of the hard-sphere fluid, which possesses complex (oscillatory) poles only.

Returning now to figure 1, we note that the dominant pole or poles are, for both densities, well separated from the others. This suggests, following [2], that the contributions from

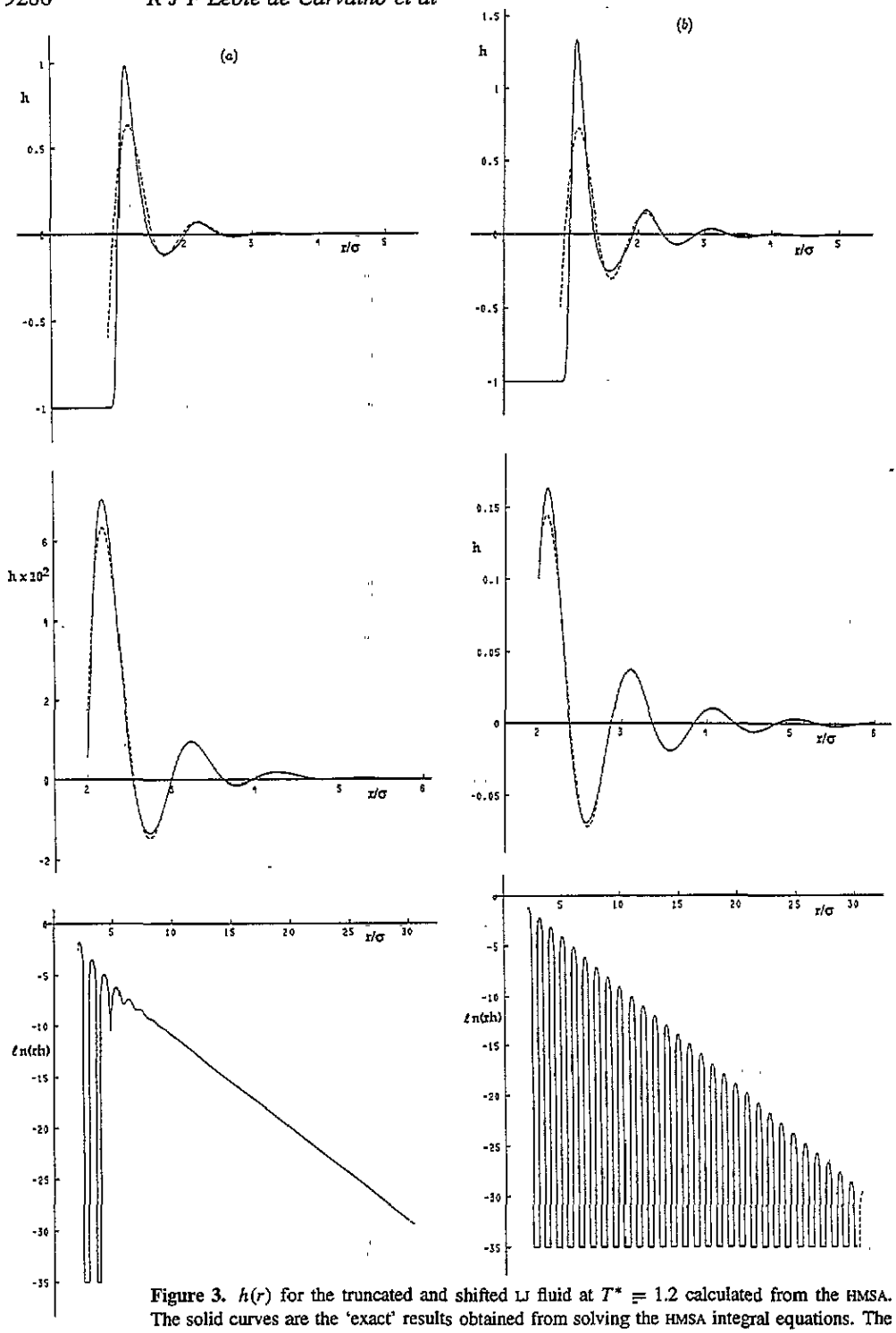

Figure 3. $h(r)$ for the truncated and shifted LJ fluid at $T^* = 1.2$ calculated from the HMSA. The solid curves are the 'exact' results obtained from solving the HMSA integral equations. The dashed curves are asymptotic results retaining the single pole on the imaginary axis plus the leading conjugate pair of complex poles—see figure 1. (a) $\rho^* = 0.445$. The pure imaginary pole has $\alpha_0\sigma = 0.9019$ and the conjugate pair has $\alpha\sigma = \pm 6.0685 + i1.6041$. (b) $\rho^* = 0.715$. Now the pure imaginary pole has $\alpha_0\sigma = 1.9472$ and the conjugate pair has $\alpha\sigma = \pm 6.4265 + i1.0041$. The second figure in each set shows the results on an expanded vertical scale while the third is a plot of $\ln(rh(r))$ versus r (the asymptotic results lie on the top of the 'exact'). Note that in (a) the ln plot is a straight line for large r, indicating pure exponential decay at longest range, whereas in (b) exponentially damped oscillations persist for all r.

these poles should determine the intermediate-range structure as well as the asymptotics of $h(r)$. In figure 3 we compare our numerical results for $h(r)$, the full solution of the HMSA, with those of the pole analysis. Only the contributions from the pure imaginary and the first conjugate pair of complex poles are retained. Figure 3(a) corresponds to the poles in figure 1(a), the lower-density state, and figure 3(b) to those in figure 1(b), the higher-density state. (The values of α for the poles which are retained are given in the captions.) For both densities we show results on three scales. The fit to the 'exact' results is very good for $r > 2\sigma$ at both densities. For $r \gtrsim 3\sigma$ the results of the leading-order pole analysis are indistinguishable from the 'exact' results at normal magnification. In the final plots of figure 3(a) and figure 3(b) we show $\ln(rh(r))$ versus r. At the lower density the oscillations have disappeared for $r \gtrsim 10\sigma$; i.e., the ultimate decay is purely exponential since the pure imaginary pole has the smaller α_0. By contrast, at the higher density, $rh(r)$ remains exponentially damped oscillatory for all r since the conjugate pair of complex poles has the smaller α_0.

The quality of the fits from the pole analysis is similar to that found in [2] for the square-well fluid treated in the RPA. This suggests that (a) leading-order asymptotics are just as useful for soft-core potentials as they are for hard-core potentials and (b) the quality of the fit found in [2] was not an artifact of the use of the RPA. We have not attemped to improve the fit to the 'exact' result by including further pole contributions. Since the higher-order poles are clustered (they have similar values of α_0—see figure 1) this is unlikely to provide a useful route to short-ranged structure. Note that both the HNC and the HMSA generate complex poles with $0 < |\alpha_1| < 2\pi/\sigma$. This does not occur in the RPA treatment of the square-well fluid [2], where $|\alpha_1| \gtrsim 2\pi/\sigma$ for all complex poles †. Finally we should remark that, for all state points we have considered, we find only a single pure imaginary pole in both the HNC and HMSA calculations. In [2] (section III) we gave an argument as to why at most one imaginary pole should be expected for a $c(r)$ which is of finite range. That argument required that if $c^{(2)} > 0$ then all the other moments $c^{(2n)}$ of $c(r)$, with $n \geqslant 2$, should be positive. This requirement should still be met within the HNC or HMSA where $c(r)$ is no longer finite ranged but decays with a positive tail—see (31).

3.2. Long-ranged case

In this subsection we present results for the asymptotics of $h(r)$ for a simple model treated in the RPA. We consider a system characterized by the following long-ranged pair potential:

$$\begin{aligned} \phi(r) &= +\infty \qquad && r \leqslant \sigma \\ &= -\epsilon \qquad && \sigma < r \leqslant \tfrac{3}{2}\sigma \\ &= -\frac{a_6}{r^6} \qquad && \tfrac{3}{2}\sigma < r \end{aligned} \tag{33}$$

where $a_6, \epsilon > 0$ and for continuity at $r = \frac{3}{2}\sigma$, we choose $a_6 = \epsilon\left(\frac{3}{2}\sigma\right)^6$. The RPA for this fluid is defined by

$$c(r) = c_{\mathrm{hs}}(r) - \beta\phi_{\mathrm{att}}(r) \tag{34}$$

† However, it does occur in the RPA for potentials of the form (33, 37) for both small ($R = 2.5\sigma$) and large cut-off—see figure 4.

where $c_{hs}(r)$ is the direct correlation function of a hard-sphere fluid of diameter σ and ϕ_{att} is the attractive part of the potential

$$\begin{aligned} \phi_{att}(r) &= -\epsilon \qquad r \leqslant R_c \\ &= -\frac{a_6}{r^6} \qquad R_c < r \end{aligned} \tag{35}$$

with $R_c \equiv 3\sigma/2$. The major defect of the RPA is that $g(r)$ as obtained from the OZ equation (2) does not vanish identically inside the hard-core $r < \sigma$. For our present purposes, however, it has the merit of yielding an explicit form for $\hat{c}(q)$ which enables us to calculate the poles of $\hat{h}(q)$ and test the accuracy of the asymptotic formula (23). We employ the Percus–Yevick approximation for $c_{hs}(r)$ so $\hat{c}_{hs}(q)$ is known analytically. By Fourier transforming (35), we find after some algebra

$$\beta\hat{\phi}_{att}(q) = -4\pi\epsilon\beta\left[\sin(qR_c)\left(\frac{1}{q^3}+\frac{R_c^2}{4q}-\frac{R_c^4 q}{24}\right)+\cos(qR_c)\left(-\frac{R_c}{q^2}+\frac{R_c^3}{12}-\frac{q^2R_c^5}{24}\right)\right]$$
$$+\frac{\pi\epsilon\beta R_c^3}{6}\sum_{n=0}^{\infty}\frac{(-1)^n(qR_c)^{2n+4}}{(2n+1)(2n+1)!}-\frac{\pi^2\epsilon\beta R_c^6}{12}q^3. \tag{36}$$

Since $\hat{c}_{hs}(q)$ is an analytic function of q^2 it follows that $\hat{c}(q) = \hat{c}_{hs}(q) - \beta\hat{\phi}_{att}(q)$ has the desired form (13), with $\hat{c}^{sr}(q)$ defined as the sum of $\hat{c}_{hs}(q)$ and all terms except the q^3 term in $-\beta\hat{\phi}_{att}(q)$. The resulting $\hat{c}^{sr}(q)$ has the required power-series expansion (15). Note that the coefficient a of the q^3 term in (13) is given by $a = \beta\pi^2\epsilon R_c^6/12$ in the RPA treatment. As expected, this agrees with the exact result (14) for this coefficient ($a_6 = \epsilon R_c^6$ for the present model potential) since the RPA enforces the condition $c(r) \to -\beta\phi(r)$, as $r \to \infty$. The critical temperature and density, obtained from the compressibility route, i.e., from $\hat{c}(0)$, are $k_B T_c/\epsilon = 2.533$ and $\rho_c\sigma^3 = 0.246$, respectively.

In addition to the long-ranged potential we consider a set of truncated and shifted potentials constructed from (33)

$$\begin{aligned} \phi_T(r) &= \epsilon_T\,(\phi(r) - \phi(R)) \qquad r \leqslant R \\ &= 0 \qquad r > R \end{aligned} \tag{37}$$

R is the cut-off distance and ϵ_T is a dimensionless constant chosen so that the compressibility and related thermodynamic properties are the same as those for the long-ranged potential (i.e., $\hat{c}_T(0) = \hat{c}(0)$). The truncated systems are also treated in the RPA and hence all the models possess the same mean-field liquid–vapour coexistence curve. Since $c(r)$ is finite ranged the poles can be calculated using (9) and (10). We concentrate first on results for truncated potentials with increasing values of R.

In figure 4 we plot the poles for truncated potentials, at density $\rho^* \equiv \rho\sigma^3 = 0.8$ and temperature $T/T_c = 1.18$ where T_c is the critical temperature of the full model (33). The circles correspond to the poles at $R = 2.5\sigma$. These poles are all well separated and the sequence is somewhat similar to that found for the square-well fluid treated in the RPA (see figure 2 in [2]). At this state point the medium-range and asymptotic correlations are

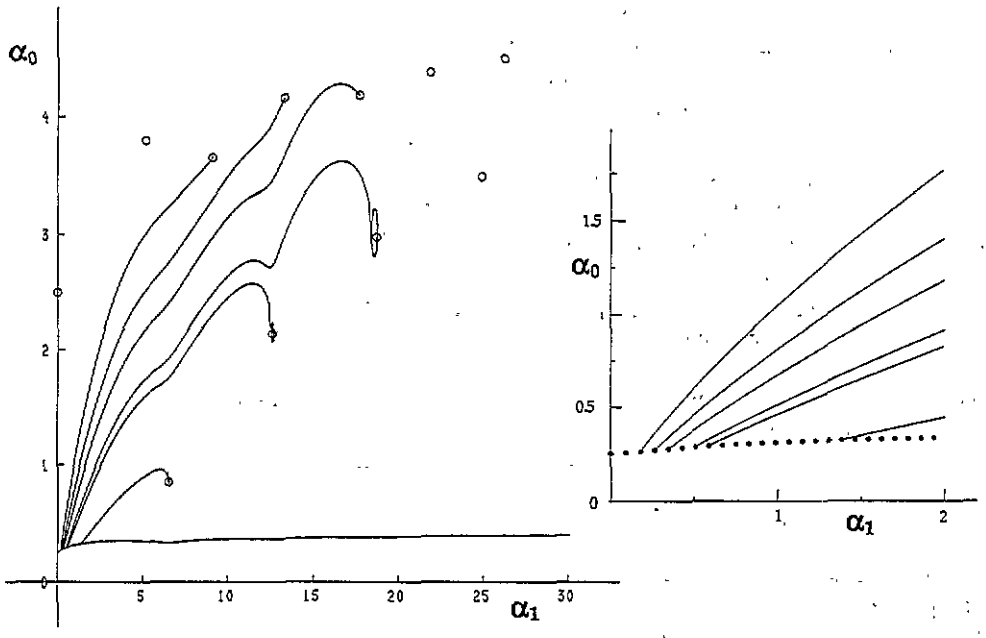

Figure 4. The poles of $\hat{h}(q)$ calculated from the RPA for various reference fluids, all at $T/T_c = 1.18$ and $\rho^* = 0.8$ (see text). The circles refer to a cut-off $R = 2.5\ \sigma$ and the bottom dotted line to $R = 80\sigma$. The solid lines show the trajectories of six poles plotted for values of R in the range $2.5\ \sigma \leqslant R \leqslant 80\sigma$. As R increases the poles cluster at a small value of α_0—see the inset, which plots the trajectories and displays the poles for $R = 80\sigma$ (dots) on an expanded scale. Poles off the imaginary axis occur in conjugate pairs (see caption to figure 1).

determined by a conjugate pair of complex poles lying at $\alpha_1 \approx \pm 2\pi/\sigma$. For this fluid there is a well defined FW line; i.e., at some lower density the pure imaginary pole has the same α_0 as the conjugate pair. We calculated the trajectories of poles as the cut-off distance was increased from 2.5σ to 80σ. For clarity, in figure 4, these are shown for six poles only. As R is increased the trajectories of certain poles spiral at first before clustering along the dotted line which denotes the results for $R = 80\sigma$. The pole on the imaginary axis is now associated with the ultimate exponential decay beyond the range of the potential (80σ) and the amplitude of its contribution to $rh(r)$ is markedly reduced at this large value of R. A reasonable description of intermediate-range correlations requires a rapidly increasing number of poles as the cut-off distance R is increased. For large R the poles are no longer well separated and a pole analysis is not of practical use. At first sight the contrast between the distribution of poles for $R = 2.5\sigma$ and 80σ seems quite dramatic when one considers that the potentials for these two cases are not substantially different—the extra tail contribution is very small. For example, there is no pronounced signature of a dominant conjugate pair of complex poles near $\alpha_1 = \pm 2\pi/\sigma$ when R is very large. Moreover, as R is increased the FW crossover, at fixed T, shifts towards higher densities and soon loses the physical significance it has for short cut-off potentials. However, on further consideration one realizes that for large R the pole analysis, which expands $rh(r)$ as a set of (complex) exponentials, is attempting to describe the inverse power-law decay which characterizes the correlation functions inside much of the range of the truncated potential. This is the basic

reason why one requires an impracticable number of terms in the pole expansion.

We return then to the full, long-ranged potential (33). In this case the leading pole was determined numerically by calculating the imaginary and real parts of the complex function of complex variable q, $f(q) \equiv 1 - \rho\hat{c}(q)$, with $\hat{c}(q)$ given by the RPA, (34)–(36). For each state point we took the leading complex pole of the system (37) truncated at $R = 2.5\sigma$ as an initial guess. By varying α_0 and α_1 we could, by trial and error, find the pole of the full system, that is, determine the intersection of $\mathrm{Re}\left[f(q)\right] = 0$ with $\mathrm{Im}\left[f(q)\right] = 0$. In the calculations, the series expansion in (36) was truncated at $n = 15$. Results for $h(r)$ are presented in figure 5 for two densities at temperature $T/T_c = 1.18$. For $\rho^* = 0.8$ there is a pole at $\alpha_1 + \mathrm{i}\alpha_0 = 6.489\,60 + \mathrm{i}0.858\,05$. The corresponding conjugate pair of poles for the reference system, truncated and shifted at $R = 2.5\sigma$, are $\pm 6.480\,00 + \mathrm{i}0.851\,80$. For $\rho^* = 0.45$ the leading-order pole is at $\alpha_1 + \mathrm{i}\alpha_0 = 5.594\,28 + \mathrm{i}1.586\,15$ for the full potential and at $\pm 5.554\,77 + \mathrm{i}1.602\,27$ for the reference potential. We checked numerically that for the full long-ranged potential (33) there are no poles on the imaginary axis. Figures 5(a) and 5(b) compare the 'exact' $h(r)$ with the asymptotic form

$$rh(r) \sim |A|\,\mathrm{e}^{-\alpha_0 r}\cos(\alpha_1 r - \theta) + S^2(0)\beta\frac{a_6}{r^5} \tag{38}$$

obtained by retaining only the leading-order-pole contribution and the slowest power-law decay in (23). The 'exact' result was calculated by numerical Fourier inversion of $\hat{h}(q) = \hat{c}(q)/(1 - \rho\hat{c}(q))$ with $\hat{c}(q)$ obtained by numerical Fourier transform of the RPA $c(r)$, truncated at $r = 80\sigma$†. We checked that such a procedure provides a very accurate $h(r)$ for r up to about 50σ, before the cut-off effect becomes noticeable, which is ample for the present purpose. For $\rho^* = 0.8$ (figure 5(a)) the agreement is excellent for distances larger than $r \approx 2.2\sigma$. The second plot in figure 5(a) shows clearly that intermediate-range structure is described almost perfectly by the leading pole. At $r \approx 25\sigma$ the leading power-law tail becomes comparable to the pole contribution and dominates completely for $r \gtrsim 35\sigma$. At this density it is clear that the poles are well separated and that the higher-order power-law contributions are small compared to the leading r^{-6} term. At $\rho^* = 0.45$ the poles remain well separated and figure 5(b) shows that (38) provides an excellent fit to $h(r)$ for $2\sigma \lesssim r \lesssim 6\sigma$. However, the high-order power-law contributions are non-negligible for $r \gtrsim 6\sigma$ and the ultimate r^{-6} term does not dominate fully until $r \gtrsim 40\sigma$. Note that now α_0 is nearly twice as large as for $\rho^* = 0.8$ so the oscillations are much more strongly damped. Moreover, the power-law contributions have larger amplitudes ($S^2(0)$ is much larger at this density) so they erode the oscillations at much shorter distances than is observed at the higher density.

The leading-order complex pole of the truncated reference system, with $R = 2.5\sigma$, lies very close to that of the full long-ranged potential— see the results quoted above. At both densities, α_0 and α_1 lie within 1% of their values for the full potential. The amplitudes $|A|$ and phases θ, calculated from the residues, are also within 1% at $\rho^* = 0.8$, although the agreement is about ten times poorer at $\rho^* = 0.45$. These results imply that the *intermediate*-range structure of $h(r)$ should be almost identical for both types of fluid. This is confirmed by comparing 'exact' results for the truncated reference potential with those of figure 5. At the higher density the results for $r \lesssim 22\sigma$ cannot be distinguished (at the present magnification) from those in figure 5(a). Only the longer-range behaviour is different: $\ln(rh(r))$ for the reference fluid continues to exhibit oscillations—see figure 3(b).

† Whilst $\hat{c}(q)$ is known analytically, this procedure was less susceptible to round-off error.

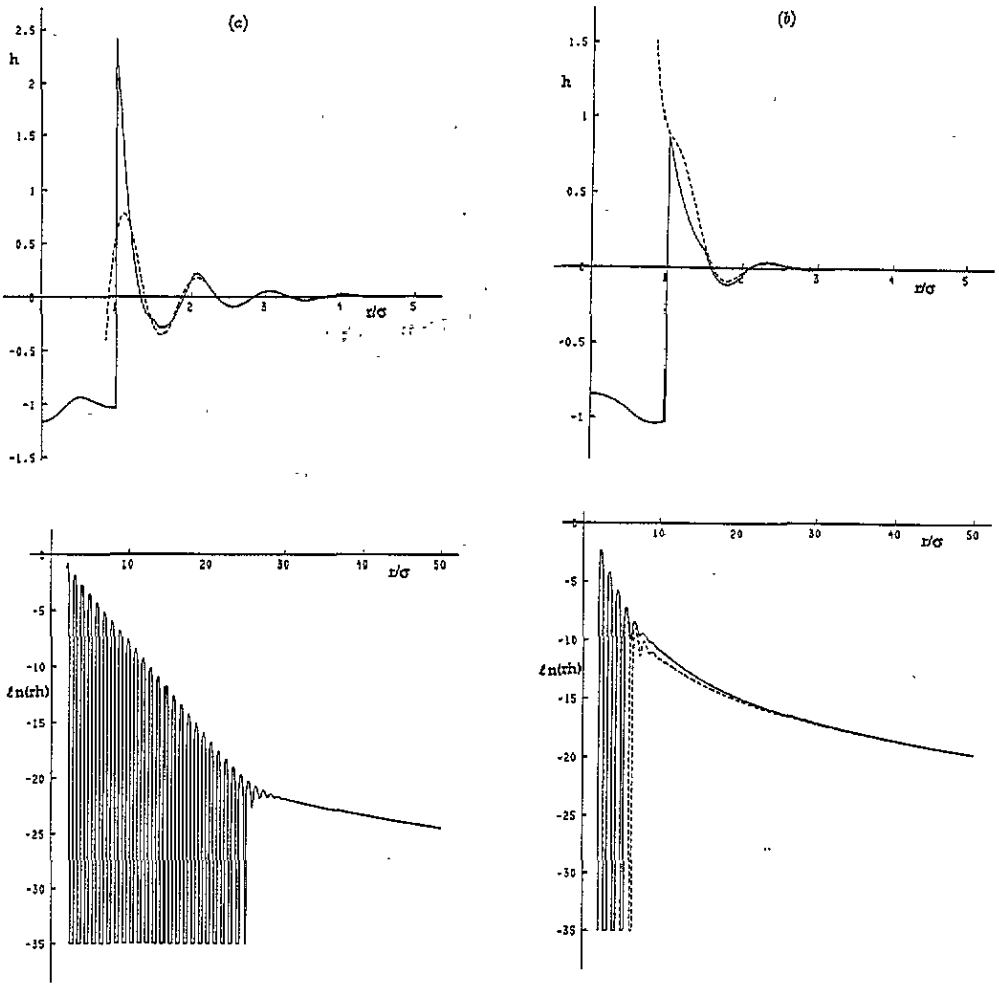

Figure 5. $h(r)$ for the full long-ranged potential (33) at $T/T_c = 1.18$ calculated from the RPA. The solid curves are the 'exact' results obtained by numerical Fourier transform of the OZ relation. The dashed curves are the asymptotic result (38) retaining the single complex pole plus the leading-order power-law contribution. (a) $\rho^* = 0.8$ and (b) $\rho^* = 0.45$. The second figure in each set shows $\ln(rh(r))$ versus r and in case (a) the asymptotic results lie on top of the 'exact' results. In (a) the decay is exponentially damped oscillatory until $r \sim 25\sigma$ when power-law decay takes over. In (b) oscillations are eroded much earlier but the ultimate r^{-6} decay does not fully dominate higher-order power-law terms until $r \gtrsim 40\sigma$.

At $\rho^* = 0.45$ the results for $r \lesssim 5\sigma$ are extremely close to those in figure 5(b). As the density $\rho^* = 0.45$ lies on the low-density side of the FW line for the reference fluid (this has a pure imaginary pole) the ultimate decay of $rh(r)$ is pure exponential (see figure 3(a)) rather than power law. Although the system with the full potential does not possess a sharp FW line, it is clear from figure 5 that the intermediate-range structure of $h(r)$ does exhibit a pronounced change of character as the density is reduced. The crossover from oscillatory to monotonic behaviour in the range $5\sigma \lesssim r \lesssim 20\sigma$ is much the same as that found for the short-ranged reference fluid, which does possess a sharp FW line, cf figure 3(a) and 3(b).

4. Discussion

Our HMSA calculation of the FW line for the truncated and shifted LJ fluid was performed for comparison with that of [3], obtained for the square-well fluid in the crude RPA. Of particular note is the fact that both sets of results show the FW line intersecting the liquid branch of the liquid–vapour coexistence curve at the same (scaled) temperature: $T/T_c \approx 0.9$, and at a similar (scaled) density: $\rho/\rho_c \approx 1.9$. Thus, in the absence of some unlikely cancellation of effects, we might conclude that neither the choice of short-ranged potential nor the accuracy of the liquid-state integral-equation theory severely affects the intersection. This means that the conclusions drawn in [3] for the square-well fluid, namely that damped oscillations should occur in the density profiles of the liquid–vapour interface for $T/T_c \leqslant 0.9$, should remain valid in an accurate theory of correlations for fluids with short-ranged potentials. The existence of oscillatory profiles on the liquid side of the interface has important repercussions for wetting phenomena: at mean-field level complete wetting of a substrate–vapour interface by an infinitely thick film of liquid can only occur on the monotonic side of the FW line [4]. The differences between the results for the present model and those for the square-well fluid [3] affect the location of the FW line only at very high temperatures, well above T_c.

Our study of the consequences arising from the inclusion of power-law interactions raises a variety of issues. Firstly, there is no sharp FW line belonging to the full model that will describe crossover of correlation-function decay either asymptotically or at intermediate range. This conclusion follows from the fact that in the presence of power-law interactions there can be no pole lying on the imaginary axis. That is, there is no longer a pure exponential contribution to $rh(r)$. However, there remains a damped oscillatory pole structure of the same type as found in typical short-ranged models. In fact, in the RPA at least, we were able to give a prescription for generating an associated truncated model whose leading-order oscillatory pole lay within 1% of the pole belonging to the full model. The associated amplitudes and phases are similarly close. In principle, these criteria could be used to define an optimum truncation length and for the state points we consider, this would be about 2.75σ. Accordingly, on the damped oscillatory side of the FW line of the truncated model, the asymptotic structure of the truncated system, given by the leading-order pole, provides a highly accurate description of the intermediate-range oscillatory structure of the full system. At lower densities the erosion of intermediate-range oscillatory structure occurs by a different mechanism in the presence of power-law interactions, namely, the power-law tail grows (with an amplitude controlled by the compressibility) as the damped oscillatory tail shrinks. Such a scenario, which was proposed in our earlier paper [2], is confirmed by the present analysis. Note that results for $h(r)$ extracted from neutron-diffraction data along the saturated liquid curves of Ne and Xe show intermediate-range damped oscillatory decay does persist up to high temperatures [21]. Only for $T/T_c > 0.95$ does the oscillatory decay seem to disappear.

From our analysis of the pole structure obtained with finite-ranged models using very long truncation lengths (possible candidates for modelling long-range potentials) we were able to identify the physical significance of the pure imaginary pole. This can only describe the ultimate exponential decay beyond the truncation range. It follows that a pole analysis of models truncated at very long range is of little practical value because the physically relevant correlations are then forced to be described entirely in terms of complex poles. As a result one finds a dense line of complex poles bearing little relation to the pole structure of the true system, in marked contrast to that of the more appropriate short-ranged reference systems described above.

It is straightforward to extend the analysis of subsection 2.2 to potentials which include $-a_8/r^8$, $-a_{10}/r^{10}$ etc terms. These give rise to q^5 and q^7 terms in $\hat{c}(q)$. One can readily

extend the procedure based on (18) to argue that there should still be no pure imaginary solution of $1 - \rho\hat{c}(q) = 0$. The higher-order power-law potentials simply make further power-law contributions to the tail of $h(r)$. Their inclusion will shift the location of the leading-order complex pole, but only slightly so that intermediate-range oscillatory structure will be little affected. Incorporating retardation effects is more complicated since these replace the q^3 term by one in $q^4 \ln q$ [12]. Nevertheless, one would again expect the leading-order complex pole to be essentially unaffected. Locating the poles is, of course, a non-trivial business. We were able to find these because we had an explicit form for $\hat{c}(q)$, obtained from the RPA. In a more sophisticated theory, where no such form is available, it is not clear how one could locate the poles. (Recall that (9) and (10) do not exist for power-law potentials†). This problem warrants further study.

As a final remark we mention a consequence of our results for the decay of pairwise correlations $h_{ij}(r)$ in real fluid mixtures where dispersion forces are present. The ultimate (power-law) decay of the $h_{ij}(r)$ will depend on the precise form of the coefficients $a_{ij}(r)$ describing the strength of the $-1/r^6$ potential between an atom of species i and one of species j, i.e., on the choice of mixing rule. However, as first pointed out by Martynov [22] and explained in [2], since the poles of all the $\hat{h}_{ij}(q)$ are determined by zeros of a common denominator the damped oscillatory contributions to $h_{ij}(r)$ will have the same exponential decay length α_0^{-1} and wavelength $2\pi/\alpha_1$ for all ij combinations. Moreover, for a binary mixture, simple amplitude and phase relations, which do *not* depend on the choice of mixing rules, relate the leading oscillatory decay of $h_{ab}(r)$ to that of $h_{aa}(r)$ and $h_{bb}(r)$ [2]. Our present work shows that for a power-law potential the leading-order complex pole is well separated from the others so its contribution dominates the intermediate-range decay of $h(r)$, providing, at high densities, an excellent fit for the range $2\sigma \leqslant r \leqslant 25\sigma$. If there are well separated pole structures for binary mixtures (which we expect) it follows that the remarkable relations for the decay of $h_{ij}(r)$ mentioned above should hold over a similar, intermediate, range. This leads to considerable simplification in the interpretation of structural data.

Acknowledgments

We have benefited from discussions of asymptotics with J H Hannay and C J Howls. RJFLdC is grateful to JNICT/Ciência (Portugal) for financial support.

References

[1] Evans R, Hoyle D C and Parry A O 1992 *Phys. Rev.* A **45** 3823 and references therein
[2] Evans R, Leote de Carvalho R J F, Henderson J R and Hoyle D C 1994 *J. Chem. Phys.* **100** 591
[3] Evans R, Henderson J R, Hoyle D C, Parry A O and Sabeur Z A 1993 *Mol. Phys.* **80** 755
[4] Henderson J R 1994 *Preprint*
[5] Henderson J R and Sabeur Z A 1992 *J. Chem. Phys.* **97** 6750; 1994 *Mol. Phys.* **82** 765
[6] Fisher M E and Widom B 1969 *J. Chem. Phys.* **50** 3756
[7] Widom B 1964 *J. Chem. Phys.* **41** 74
[8] Enderby J E, Gaskell T and March N H 1965 *Proc. Phys. Soc.* **85** 217
[9] Verlet L 1968 *Phys. Rev.* **165** 201
[10] Attard P 1993 *Phys. Rev.* E **48** 3604

† Martynov [22] attempts to derive a result akin to (23). However, he does not properly identify the (complex) exponential terms.

Ennis J 1993 *PhD Thesis* Australian National University
Ennis J, Kjellander R and Mitchell D J 1994, *J. Chem. Phys.* at press
Kjellander R and Mitchell D J 1992 *Chem. Phys. Lett.* **200** 76
Kjellander R and Mitchell D J 1994 *J. Chem. Phys.* **101** 603
Leote de Carvalho R J F and Evans R 1994 *Mol. Phys.* at press
[11] See, for example, Hansen J-P and McDonald I R 1986 *Theory of Simple Liquids* 2nd edn (New York: Academic)
[12] Reatto L and Tau M 1992 *J. Phys.: Condens. Matter* **4** 1
[13] Evans R and Sluckin T J 1981 *J. Phys. C: Solid State Phys.* **14** 2569
[14] Lighthill M J 1958 *Introduction to Fourier Analysis and Generalized Functions* (Cambridge: Cambridge University Press)
[15] Smit B 1992 *J. Chem. Phys.* **96** 8639
[16] Weeks J D, Chandler D and Andersen H C 1971 *J. Chem. Phys.* **54** 5237
[17] Zerah G and Hansen J-P 1986 *J. Chem. Phys.* **84** 2336
[18] Caccamo C, Giaquinta P V and Giunta G 1993 *J. Phys.: Condens. Matter* **5**, Supplement 34B, B75 and private communication
[19] Abramo M C and Caccamo C 1992 *Phys. Lett.* **166A** 70
[20] Cheng A, Klein M L and Caccamo C 1993 *Phys. Rev. Lett.* **71** 1200
[21] Bellissent-Funel M C, Buontempo U, Filabozzi A, Petrillo C and Ricci F P 1992 *Phys. Rev.* B **45** 4605
[22] Martynov G A 1992 *Fundamental Theory of Liquids: Method of Distribution Functions* (Bristol: Hilger) section 5.5